A Subspace Approach to Adaptive Narrow-Band Interference Suppression in DSSS

Habib Fathallah, *Student Member, IEEE,* and Leslie A. Rusch, *Member, IEEE*

***Abstract*—In this paper we address the problem of suppression of a digital narrow-band interferer in direct-sequence spread spectrum (DSSS) communications. We focus on the adaptive suppression method proposed by Honig, Madhow, and Verdú [1] for wide-band interference, applying it to a narrow-band interferer. We identify the eigenspaces of the system dynamics to analyze the convergence of the adaptive version of the minimum mean square error (MMSE) algorithm for this application. Using this subspace approach we are able to: 1) significantly decrease convergence times via a new constraint on step size in adaptation; 2) introduce a simple parameterization of the mean output energy (MOE) and signal-to-interference ratio (SIR) to compare performance of various receivers; and 3) identify modes of operation where the algorithm will cease to effectively cancel interference. We propose a new adaptive receiver that avoids the convergence anomalies identified, while capitalizing on the new step size for faster convergence. Simulation results to support theoretical results are presented.**

***Index Terms*— Blind adaptation, CDMA, direct-sequence spread spectrum communication, multiuser detection, narrow-band interference suppression, subspace analysis.**

I. Introduction

DUE TO THE scarcity of frequency allocations for emerging personal communications services, it has been proposed that spread spectrum (SS) signals be used in such services so that they can be overlaid on existing frequency band occupants [2]. Such SS signals would be constrained in power so as not to interfere with preexisting narrow-band users. For a single SS user in an additive white Gaussian noise (AWGN) channel, the optimal receiver is a filter matched to the signature sequence of the SS signal. The presence of narrow-band users makes the environment decidedly non-AWGN, especially as narrow-band users can be expected to be much more powerful than SS users. To compensate for this, many schemes have been proposed to filter out such narrow-band signals before going on to match-filter the received waveform [3].

Recent research has investigated the application of multiuser detection theory [4]–[6] to a system of one true SS user and one digital narrow-band user. We adopt the model of [6] where each interfering bit is interpreted as a virtual SS user. Suppose we have m narrow-band bits occurring in the time of a single SS bit. This can be interpreted as a code-division multiple-access (CDMA) system with $m+1$ users. Multiuser detection theory gives us an optimal and many suboptimal receivers for such a system [7]. These receivers require information on some, or perhaps all, of the following parameters: signature sequences, received energies, timing delays, etc. of all users. We focus on the blind multiuser detection algorithm proposed by Honig, Madhow, and Verdú [1], which only requires knowledge of the spreading code of the desired user (in our case, the true SS user). We exploit the structure of the virtual CDMA system to analyze this detector.

We first consider three fixed receivers. The matched filter (MF) or conventional receiver is optimal for one spread spectrum signal in AWGN and requires knowledge of the SS user's spreading code. Due to the simplicity of this receiver it is frequently used even when there are many SS users present, despite its decidedly suboptimal performance. The second receiver we consider is the decorrelating receiver, a linear receiver with asymptotic optimality characteristics [7]. This receiver requires knowledge of all users' spreading codes and timing delays, but is independent of the user powers. We also calculate the minimum mean square error (MMSE) receiver for our virtual CDMA system, reported simultaneously in [4] and [5].

The brunt of our analysis is placed in examination of the signal space and how various receivers project energy in this space. We examine the eigenspaces of the received signal's covariance matrix to partition the signal space in three subspaces Γ_{NO}, $\Gamma_{I\&N}$, and Γ_E. The eigenspace Γ_{NO} contains contributions from the noise only, and $\Gamma_{I\&N}$ from both interference and noise. Γ_E is a two-dimensional subspace which contains all of the energy of the desired signal and a subset of the interference and noise energies. This is an unexpected result as in a general system of $m+2$ users, Γ_E would have dimension $m+2$. We show that for this virtual CDMA system, the three fixed receivers of interest all project the received signal onto this two-dimensional subspace. Subspace analysis of systems with wide-band interference has not identified this two-dimensional space, but has always involved much higher dimensional spaces. By identifying this space we are able to parameterize the receivers of interest by a single variable. This parameterization allows an alternate derivation of the MMSE receiver and also allows us to see the effect of weak interference on the mean output energy

Paper approved by S. L. Miller, the Editor for Spread Spectrum of the IEEE Communications Society. Manuscript received April 18, 1996; revised January 3, 1997 and July 7, 1997. This work was supported by the Natural Sciences and Engineering Research Council of Canada and Québec-Téléphone. This paper was presented in part at GLOBECOM'96, London, U.K., 1996, and at the Interference Rejection and Signal Separation in Wireless Communications Symposium, Newark, NJ, March 19, 1996.

The authors are with the Department of Electrical and Computer Engineering, Université Laval, Sainte-Foy, P.Q. G1K 7P4, Canada (e-mail: fhabib@gel.ulaval.ca; rusch@gel.ulaval.ca).

Publisher Item Identifier S 0090-6778(97)09079-X.

(MOE). Because the space is of low dimension, we are able to improve the criteria on the step size for stability in the adaptive algorithm which searches for the MMSE solution. We propose a new limit on the step size that allows for much faster convergence. The adaptive version of the MMSE receiver minimizes the MOE via a gradient descent. Using our single parameter model of the MOE, we identify an anomaly in the convergence for weak interferers. We show that while the MOE is always convex, it is extremely shallow for weak interference signals. The algorithm will not be trapped by local minima; however, it is easily lead astray by spurious noise samples. Finally, we propose a new adaptive receiver that avoids the convergence anomalies while capitalizing on the new step size for faster convergence.

A. Overview

We begin in the following section with a simple system model describing our interpretation of the digital interferer and SS signal as a virtual CDMA system. In Section II we outline our subspace approach for three fixed receivers, while in Section III we go on to apply these results to the dynamics of the blind adaptive receiver. We identify a new less restrictive stability constraint on the step size, leading to much faster convergence. We identify certain convergence anomalies and propose a new receiver to avoid them. We present simulation results for the fixed and adaptive receivers in Section IV. Concluding remarks are given in Section V. Finally, two appendixes present details of the eigenspace analysis.

B. System Model

We consider the system model of Rusch and Poor [6] with one SS signal and one digital narrow-band signal in an otherwise AWGN channel with variance σ^2. Each data bit of the SS user has duration T and is modulated by a unit energy pseudonoise signature sequence $s_0(t)$, which spreads the signal in the frequency domain. Let m be the number of the narrow-band bits occurring during each bit of the SS user. The narrow-band signal and the SS signal are asynchronous; therefore, we will have only partial narrow-band bits at the beginning and end of the SS spreading code. In Fig. 1 we present the set of $m+1$ virtual signature sequences and the SS spreading code. The first virtual user's signature sequence is constant during the first narrow-band user's bit interval and zero everywhere else. Similarly, each narrow-band user's bit can be thought of as a signal arising from a virtual user with a signature sequence with only one nonzero interval. These form a set of orthogonal users, uncorrelated with one another. However, in general, the ith virtual user's signature sequence $s_i(t)$, taken to have unit energy, will have some cross correlation ρ_i with the spread spectrum user $\rho_i = \int_0^T s_0(t)s_i(t)\,dt$ for i from 1 to $m+1$, forming the vector ρ.

We assume that the received signal strength for both signals remains constant for the SS bit interval, i.e., a slowly varying channel. Let w_I be the received energy of the narrow-band signal, and w_0 the received energy of the SS user. We will use the notation that the narrow-band user bipolar data bits during the interval $(0,T)$ are $b_1,\cdots,b_{m+1}$ or the vector $\mathbf{b}$ and the bipolar SS bit is b_0. The received signal during one bit interval of the SS user for $t \in [0,T]$ is thus

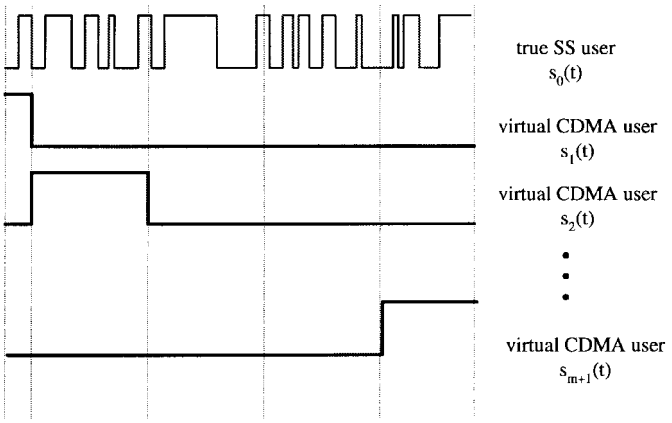

Fig. 1. Virtual CDMA system.

$$y(t) = \sqrt{w_0}b_0s_0(t) + \sqrt{w_I}\sum_{i=1}^{m+1} b_is_i(t) + \sigma n(t) \qquad (1)$$

where $n(t)$ is a unit spectral-density AWGN. Whereas a one-shot examination of the SS user is suboptimal (we are neglecting the information from one SS bit to the next), the complexity of the receiver is greatly reduced. Given that our system is only a virtual CDMA system, we lose less information (in leading and trailing bits, not in all bits) than a true CDMA system.

II. Subspace Approach for Fixed Receivers

A. Various Bases and Subspaces

We assume that we sample the received signal N times in an SS bit interval (N typically being the length of the direct-sequence spreading code). Therefore, the signature sequences can be represented as finite dimensional vectors. In this section we define three sets of basis vectors for Γ, the space (dimension N) spanned by all possible signature sequence vectors. The set of standard basis vectors we call B_e, with the definition

$$e_j[i] = \begin{cases} 1, & i=j \\ 0, & i\neq j. \end{cases}$$

The space spanned by all active signature sequences we call Γ_{act}. Note that for our virtual CDMA system there are $m+2$ active users, therefore Γ_{act} has dimension $m+2$. The orthogonal complement of Γ_{act} we call Γ_{NO} as it contains energy from noise only, with no energy from an active user. A second set of basis vectors for Γ_{act} is formed by the signature sequences themselves; we refer to this basis as B_s. These vectors span the space Γ_{act}, have unit length (from having unit energy), and are linearly independent, but are not orthogonal. The third set of basis vectors B_{vy} are formed from the eigenvectors of the matrix $\mathbf{R_{vy}}$ defined in Section III-A. The matrix $\mathbf{R_{vy}}$ governs the dynamics of the gradient descent algorithm. We will describe the evolution of the

algorithm using the projections of the tap weight vector onto the eigenvectors of $\mathbf{R_{vy}}$.

B. Covariance Matrix and Eigenspaces

In order to eventually generate the basis B_{vy} for Γ, we calculate the eigenvalues and eigenvectors of the covariance matrix $\mathbf{R_{yy}}$ $(N\times N)$ of the received signal. Using the standard basis for the discrete-time (sampled) version of (1), we have the following expression for $\mathbf{R_{yy}}$:

$$\mathbf{R_{yy}} = E\{\mathbf{y}\mathbf{y}^T\} = w_0\mathbf{s_0}\mathbf{s_0^T} + w_I\sum_{i=1}^{m+1}\mathbf{s_i}\mathbf{s_i^T} + \sigma^2\mathbf{I_N}.$$

We demonstrate in Appendix A that the subspace Γ_{act} is invariant with $\mathbf{R_{yy}}$ (or $\mathbf{R_{yy}}$-invariant). This allows us to define and calculate the restriction of $\mathbf{R_{yy}}$ in Γ_{act}, which we denote by

$$\tilde{\mathbf{R}}_{\mathbf{yy}} = \begin{bmatrix} w_0+\sigma^2 & w_I\rho^T \\ w_0\rho & (w_I+\sigma^2)\mathbf{I_{m+1}} \end{bmatrix}_{B_s}.$$

This matrix is diagonalized in Appendix A, facilitating the calculation of the eigenvalues and eigenvectors. For constants Δ^+, Δ^-, δ_i, and γ_i, defined in Appendix A, the orthonormal set of eigenvectors is given by

$$\mathbf{V_{0y}} = \gamma_0[\Delta^- \quad -\rho_1 \quad \cdots \quad -\rho_{m+1}]^T_{B_s} = \gamma_0[\Delta^- \quad -\rho^T]^T_{B_s}$$
$$\mathbf{V_{1y}} = \gamma_1[\Delta^+ \quad -\rho^T]^T_{B_s}$$
$$\mathbf{V_{iy}} = \gamma_i[0 \quad \rho_i\rho_1 \quad \cdots \quad \rho_i\rho_{i-1}\delta_i \quad \cdots \quad 0]^T_{B_s} \qquad \forall 2\le i\le m+1.$$

The remaining eigenvectors relative to Γ_{NO} are

$$\mathbf{V_{iy}} = \gamma_i\left(e_i - \sum_{j=0}^{i-1}\langle e_i, \mathbf{V_{jy}}\rangle\mathbf{V_{jy}}\right) \quad \forall m+2\le i<N.$$

The eigenvalues (calculated in Appendix A) associated with these eigenvectors describe the average energy of the received signal in that direction. Only the constants Δ^+ and Δ^- are functions of the desired user's power w_0. Eigenvectors $\mathbf{V_{0y}}$ and $\mathbf{V_{1y}}$ span a subspace of dimension two that we call Γ_E, as it contains all of the energy from the desired user and the *effective* energy from the interference and noise. We say effective energy, because we will show that three important fixed detectors (the MF receiver, decorrelating receiver, and MMSE receiver) project the received signal onto this subspace; therefore, it is only this subset of interference and noise energy which affects receiver performance. We should note that the decorrelating and the MMSE receivers may not project onto this space for all CDMA systems; however, we will show that for this virtual CDMA system they do, as does the adaptive version of the MMSE detector discussed in Section III-A. This subspace should not be confused with the subdivisions of Γ_{act} discussed in [8].

The set of eigenvectors for $2\le i\le m+1$ are orthogonal to $\mathbf{s_0}$ and span a space we call $\Gamma_{I\&N}$ (the orthogonal complement of Γ_E relative to the space Γ_{act}), that is, $\Gamma_{I\&N}$ and Γ_E form a partition of Γ_{act}. The remainder of eigenvectors for $m+2\le i\le N$ span the space Γ_{NO}. Note the eigenvalues associated with $\Gamma_{I\&N}$ are functions of the interference power and the noise power, while the eigenvalues associated with Γ_{NO} are functions of the noise power only. To recap the subspaces discussed, we have the relationship $\Gamma = \Gamma_{\text{NO}}\oplus\Gamma_{\text{act}} = \Gamma_{\text{NO}}\oplus\Gamma_{I\&N}\oplus\Gamma_E$ where $\oplus$ represents a direct sum. These subspaces are illustrated in Fig. 2.

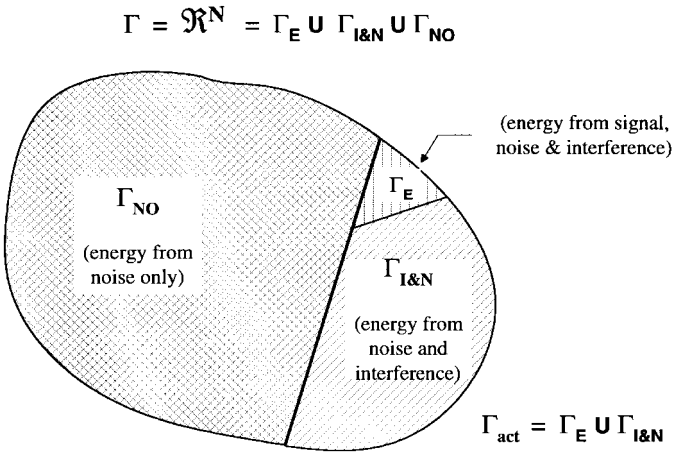

Fig. 2. Subspace partition.

The canonical form of a receiver is defined in [1] as the sum of the desired user's spreading code $\mathbf{s_0}$ plus a vector orthogonal to $\mathbf{s_0}$, i.e., $\mathbf{c} = \mathbf{s_0}+\mathbf{x_0}$. The vector $\mathbf{s_0}$ can be written as a linear combination of $\mathbf{V_{0y}}$ and $\mathbf{V_{1y}}$ (see Appendix A), and therefore falls in Γ_E. We construct a second vector $\mathbf{V}^\perp$ in Γ_E that is orthogonal to $\mathbf{s_0}$, and together they span Γ_E.

$$\begin{aligned}\mathbf{V}^\perp &= \frac{1}{\sqrt{\rho^T\rho(1-\rho^T\rho)}} \\ &\quad\cdot[\rho^T\rho \quad -\rho_1 \quad -\rho_2 \quad \cdots \quad -\rho_{m+1}]^T_{B_s} \\ &= \frac{1}{\sqrt{\rho^T\rho(1-\rho^T\rho)}}\cdot[\rho^T\rho \quad -\rho^T]^T_{B_s}. \end{aligned} \tag{2}$$

As the three fixed receivers we will examine all project the received signal onto Γ_E, the vector orthogonal to $\mathbf{s_0}$ must be a constant times the vector $\mathbf{V}^\perp$. This will allow us to parameterize these receivers by the constant multiplying $\mathbf{V}^\perp$, a constant we will call β, i.e., $\mathbf{c} = \mathbf{s_0}+\beta\mathbf{V}^\perp$.

C. MMSE, Decorrelating, and MF Detectors

The MF receiver is given by $\mathbf{c_{MF}} = \mathbf{s_0}$ so that, clearly, $\beta = 0$ in our parameterization. The decorrelating detector for the virtual CDMA system is given by [6]. In Appendix A we calculate its canonical form, arriving at

$$\begin{aligned}\mathbf{c_{DEC}} &= \frac{1}{\sqrt{1-\rho^T\rho}}\cdot[1 \quad -\rho^T]^T_{B_s} \\ &= \mathbf{s_0} + \sqrt{\frac{\rho^T\rho}{1-\rho^T\rho}}\cdot\mathbf{V}^\perp = \mathbf{s_0}+\beta_{\text{DEC}}\cdot\mathbf{V}^\perp\end{aligned}$$

which demonstrates that these two detectors do indeed fall in Γ_E. We now derive an expression for the detector which minimizes the mean square error (MSE) (reported simultaneously in [4] and [5]).

Per [1], the detector which minimizes the MSE is determined by the inverse of the matrix $\mathbf{R}+\sigma^2\mathbf{W}^{-1}$ where $\mathbf{R}$ is the cross correlation matrix and $\mathbf{W}$ is the diagonal matrix of user powers. For our system this inverse can be found explicitly as a function of the interference power, the noise power, and the cross correlation vector ρ, yielding

$$\begin{aligned}\mathbf{c_{MMSE}} &= \frac{1}{1-\rho^T\rho+\sigma^2/w_I}\cdot[(1+\sigma^2/w_I)-\rho^T]^T_{B_s}\\ &= \mathbf{s_0}+\frac{\sqrt{\rho^T\rho(1-\rho^T\rho)}}{1-\rho^T\rho+\sigma^2/w_I}\cdot\mathbf{V}^{\perp}. \qquad (3)\end{aligned}$$

This receiver decides between an SS bit of 1 or -1 by examining the following decision statistic:

$$\text{D.S.} = b_0+\frac{\mathbf{b}^T\rho\cdot\sigma^2/\alpha^2+\tilde{n}}{1-\rho^T\rho+\sigma^2/\alpha^2}$$

where the effective AWGN $\tilde{n}$ has zero mean and variance

$$\tilde{\sigma}^2=\sigma^2[(1+\sigma^2/\alpha^2)^2-(1+2\sigma^2/\alpha^2)\rho^T\rho]$$

and $\alpha=\sqrt{w_I/w_0}$, the near–far ratio. The probability of error using this decision statistic against a zero threshold is[1]

$$P_e=\frac{1}{2^{m+1}}\sum_{i=0}^{2^{m+1}-1}Q\left(\frac{1+\sigma^2/\alpha^2-\rho^T\rho-\rho^T\mathbf{b}^i\cdot\sigma^2/\alpha}{\tilde{\sigma}}\right)$$

where $\{\mathbf{b}^i\}$ is an ordering of the vectors of possible interference bits.

D. Parametrized MOE and Signal-to-Interference Ratio (SIR)

In [1], Honig *et al.* demonstrated that the receiver which minimizes the MSE also minimizes the MOE, defined as $\text{MOE}(\mathbf{c})=E\{\langle\mathbf{c},\mathbf{y}\rangle^2\}$. We now find an alternate derivation of the vector $\mathbf{c}$ which minimizes this expression, using our subspace partition. Any two vectors $\mathbf{c}$ and $\mathbf{y}$ can be decomposed into their components falling into each of the spaces Γ_E, $\Gamma_{I\&N}$, and Γ_{NO}. For the received signal $\mathbf{y}$, only the component in Γ_E will contain energy from the desired user. The component of $\mathbf{y}$ in Γ_{NO} contains only energy from the AWGN, and the component of $\mathbf{y}$ in $\Gamma_{I\&N}$ has energy only from the AWGN and the narrow-band interference. We will minimize the noise and interference energy in the output by choosing the components of $\mathbf{c_{opt}}$ in $\Gamma_{I\&N}$ and Γ_{NO} to be zero. Therefore $\mathbf{c_{opt}}$ falls in the two-dimensional space Γ_E and can be written as $\mathbf{c_{opt}}=\mathbf{s_0}+\beta_{\min}\mathbf{V}^{\perp}$. To find the value of β minimizing the MOE, we write the MOE as a function of β and differentiate

$$\begin{aligned}\text{MOE}(\beta) &= w_0\langle\mathbf{c},\mathbf{s_0}\rangle^2+w_I\sum_{i=1}^{m+1}\langle\mathbf{c},\mathbf{s_i}\rangle^2+\sigma^2\langle\mathbf{c},\mathbf{c}\rangle\\ &= w_0+\sigma^2+w_I\rho^T\rho+\beta^2(w_I(1-\rho^T\rho)+\sigma^2)\\ &\quad -2\beta w_I\sqrt{\rho^T\rho(1-\rho^T\rho)}.\end{aligned}$$

[1] $Q(x)=\frac{1}{\sqrt{2\pi}}\int_x^{\infty}e^{-v^2/2}\,dv$.

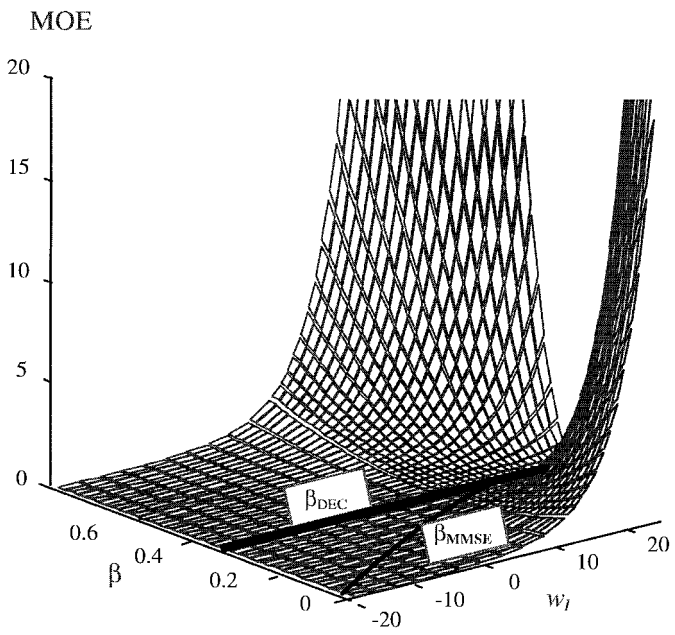

Fig. 3. MOE as a function of interference power and parameter β.

The value of β which minimizes this expression is just

$$\beta_{\min}=\frac{\sqrt{\rho^T\rho(1-\rho^T\rho)}}{1-\rho^T\rho+\sigma^2/w_I}$$

matching the previous result for the MMSE detector in (3).

In Fig. 3 we plot the MOE as a function of β and the interference power (relative to the desired user's power). The minimum of the function is traced in the plot. Note that β_{DEC} is constant and does not vary with interference power; it is also traced in the plot. The adaptive version of the MMSE receiver minimizes the MOE. As the MOE is convex in β, the algorithm will not be trapped in local minima. However, the function is much less convex as the interference power approaches the desired user's power, as is evident in Fig. 3, and is nearly flat for very weak interference. This leads us to anticipate that the adaptive algorithm will be much less effective in the presence of a weak interferer, as is demonstrated in the simulations of Section IV-C.

This parameterization β can also be used to facilitate calculation of the SIR defined as

$$\text{SIR}(\mathbf{c})=\frac{\text{signal power}}{\text{MOE}(\mathbf{c})-\text{signal power}}.$$

For the three fixed receivers, we can write this as a function of β, as shown at the bottom of the page. In Fig. 4 we plot the SIR as a function of β and the interference power. It is clear that $\beta_{\min}$ gives a peak in the SIR for high values of interference power, whereas this peak is lost for weak interferers.

$$\text{SIR}(\beta)=\frac{w_0}{\sigma^2+w_I\rho^T\rho+\beta^2(w_I(1-\rho^T\rho)+\sigma^2)-2\beta w_I\sqrt{\rho^T\rho(1-\rho^T\rho)}}$$

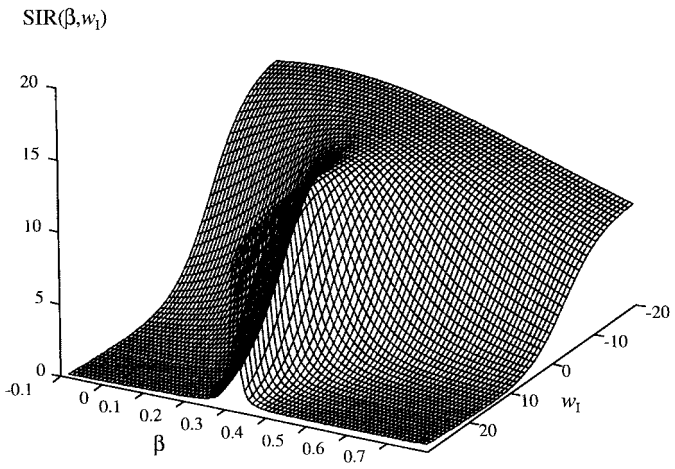

Fig. 4. SIR as a function of interference power and parameter β.

III. Subspace Approach for Blind Adaptation

In this section we examine the stochastic gradient algorithm which converges to the minimum MOE and, hence, the MMSE receiver [1]. As mentioned previously, interest in the MMSE receiver is motivated by the existence of this adaptive version. The stochastic gradient algorithm does not require information about the interfering users' power, timing, or signature sequences, nor does it require a training sequence.

We adopt the same signal space approach described previously to examine the dynamics of the adaptive algorithm. Because the interference signals are mutually orthogonal, we are able to demonstrate that the adaptive receiver is, on average, confined to the two-dimensional subspace Γ_E. This contrasts with previous analysis which isolated the receiver only within the $m+2$-dimensional space Γ_{act}. Because of this result, we are able to identify a less restrictive stability constraint on the step size in the adaptation, allowing for significantly faster convergence. The stochastic gradient is a noisy algorithm (leading to nonzero components in the noise only subspace Γ_{NO}); therefore, it is preferable to switch to a fixed receiver or decision-directed least mean squares (LMS) algorithm after nominal convergence to the MMSE receiver.

A. System Dynamics—Eigenspaces of $\mathbf{R_{vy}}$

As mentioned earlier, the receiver that minimizes the MOE also minimizes the MSE. A gradient descent algorithm was proposed to adaptively minimize the convex function MOE. This linear detector is written in the canonical form, that is, as the sum of the desired user's signature sequence plus a vector orthogonal to this signature sequence $\mathbf{c}=\mathbf{s_0}+\mathbf{x_0}$. The adaptation algorithm is

$$\mathbf{c}(n)=\mathbf{c}(n-1)-\mu\cdot\langle\mathbf{c}(n-1),\mathbf{y}(n)\rangle \cdot(\mathbf{y}(n)-\langle\mathbf{s_0},\mathbf{y}(n)\rangle\cdot\mathbf{s_0})$$

where the index n refers to the iteration or bit interval. Note that at each iteration we are scaling the projection of the received signal onto the space orthogonal to $\mathbf{s_0}$ to update the vector $\mathbf{c}$. We define the vector $\mathbf{v}(n)=(\mathbf{I_N}-\mathbf{s_0}\mathbf{s_0^T})\mathbf{y}(n)$, the product of the Householder matrix and the received signal. With this definition the algorithm can be written as

$$\mathbf{c}(n)=[\mathbf{I_N}-\mu\mathbf{v}(n)\mathbf{y}^T(n)]\mathbf{c}(n-1).$$

Taking expectations of both sides we have

$$\begin{aligned}E\{\mathbf{c}(n)\}&=[\mathbf{I_N}-\mu E\{\mathbf{v}(n)\mathbf{y}^T(n)\}]E\{\mathbf{c}(n-1)\}\\&=[\mathbf{I_N}-\mu\mathbf{R_{vy}}]E\{\mathbf{c}(n-1)\}.\end{aligned}$$

To study the dynamics of the adaptive system, we therefore examine the matrix $\mathbf{R_{vy}}$. The components of $\mathbf{R_{vy}}$ in Γ_{act} can be written in B_s as

$$[\mathbf{R_{vy}}]_{\Gamma_{\text{act}}}=\begin{bmatrix}-w_I\rho^T\rho & -(w_I+\sigma^2)\rho^T\\ w_I\rho & (w_I+\sigma^2)\mathbf{I_{m+1}}\end{bmatrix}_{B_s}.$$

In Appendix B we calculate the eigenvalues and eigenvectors of $\mathbf{R_{vy}}$. Because of the special form of the Householder matrix (see Appendix B for properties), we would expect the eigenvectors of $\mathbf{R_{vy}}$ to follow those of $\mathbf{R_{yy}}$, except those eigenvectors falling in Γ_E, i.e., in directions containing energy from $\mathbf{s_0}$. Indeed our calculations show that the two matrices have the same eigenvectors for $2\le i\le N-1$. The first two eigenvectors, on the other hand, are different

$$\begin{aligned}\mathbf{V_{0v}}&=[1+\sigma^2/w_I \quad -\rho^T]^T_{B_s}\cdot 1/\gamma_0' \quad \neq\mathbf{V}_{0y}\\ \mathbf{V_{1v}}&=[\rho^T\rho \quad -\rho^T]^T_{B_s}\cdot 1/\gamma_1' \quad \neq\mathbf{V}_{1y}\end{aligned}$$

where the constants γ_0' and γ_1' are given in Appendix B, and the associated eigenvalues are $\lambda_{0v}=0$ and $\lambda_{1v}=w_I(1-\rho^T\rho)+\sigma^2$. We make two important observations: the first eigenvector is a multiple of the MMSE receiver in (3) and the second eigenvector is the vector $\mathbf{V}^{\perp}$ defined in (2); together they span the space Γ_E. Note that these eigenvectors are not orthogonal (because $\mathbf{R_{vy}}$ is not symmetric), but that $\mathbf{V_{1v}}\perp\mathbf{s_0}$.

B. Tap Weight Trajectory and New Step Size

Having analyzed the matrix $\mathbf{R_{vy}}$, we are now prepared to follow the trajectory of the mean tap weight $\bar{\mathbf{c}}(n)=E\{\mathbf{c}(n)\}=[\mathbf{I_N}-\mu\mathbf{R_{vy}}]\bar{\mathbf{c}}(n-1)$. We will express the matrix $\mathbf{R_{vy}}$ in a basis of its eigenvectors B_{vy} to yield a diagonal form. The initial value of the tap weight is taken to be the desired user's spreading code (i.e., we initiate the algorithm with the MF receiver). Therefore, writing $\mathbf{s_0}$ in the basis B_{vy} (see Appendix B), we arrive at

$$\begin{aligned}\bar{\mathbf{c}}(n)&=[\mathbf{I_N}-\mu\mathbf{R_{vy}}]^n_{B_{vy}}\mathbf{s_0}\\&=[\mathbf{I_N}-\mu\mathbf{R_{vy}}]^n_{B_{vy}}\frac{1}{1-\rho^T\rho+\sigma^2/w_I}\\&\quad\cdot[\gamma_0' \quad -\gamma_1' \quad 0 \quad\cdots\quad 0]^T_{B_s}\\&=\frac{1}{1-\rho^T\rho+\sigma^2/w_I}\big[\text{diag}[1 \quad 1-\mu\lambda_{1v} \quad 1-\mu\lambda_{2v}\\&\quad\cdots\quad 1-\mu\lambda_{Nv}]_{B_{vy}}\big]^n\cdot[\gamma_0' \quad -\gamma_1' \quad\cdots\quad 0]^T_{B_s}\\&=\frac{1}{1-\rho^T\rho+\sigma^2/w_I}[\gamma_0' \quad -\gamma_1'(1-\mu\lambda_{1v})^n \quad 0\\&\quad\cdots\quad 0]^T_{B_s}\\&=\frac{\gamma_0'}{1-\rho^T\rho+\sigma^2/w_I}\mathbf{V_{0v}}-\frac{\gamma_1'(1-\mu\lambda_{1v})^n}{1-\rho^T\rho+\sigma^2/w_I}\mathbf{V_{1v}}.\end{aligned}$$

The mean tap weight vector falls entirely in the subspace Γ_E. Therefore, we can write its parameterized form as

$$\bar{\mathbf{c}}(n) = \mathbf{s_0} + \frac{\sqrt{\rho^T\rho(1-\rho^T\rho)}}{1-\rho^T\rho+\sigma^2/w_I} \times \left(1-\left[1-\mu\left(w_I(1-\rho^T\rho)+\sigma^2\right)\right]^n\right)\cdot \mathbf{V}^{\perp}. \quad (4)$$

Given that the $\lambda_{0v}=0$, the *only eigenvalue* that effects the stability of the algorithm is λ_{1v} so that

$$\mu < \frac{2}{w_I(1-\rho^T\rho)+\sigma^2} \quad (5)$$

ensures convergence of the mean tap vector. As n tends to infinity, (4) approaches the MMSE detector. This is a less restrictive stability constraint than the maximum eigenvalue of $\mathbf{R_{vy}}$ proposed in [1], and reproduced below for the system under consideration

$$\mu < \frac{2}{\max(|\lambda_{\mathbf{R_{vy}}}|)} = \frac{2}{w_I+\sigma^2}.$$

C. Convergence Anomalies and a New Detector

Using our subspace approach to analyze the stochastic gradient algorithm, we can examine new performance tests for the convergence of the algorithm by projecting the mean tap weights onto the three subspaces Γ_E, $\Gamma_{I\&N}$, and Γ_{NO}. Ideally the algorithm should only have a nonzero projection onto the space Γ_E and this should asymptotically approach the MMSE detector.

$$\begin{aligned}
\langle \bar{\mathbf{c}}(n), \mathbf{V_{0v}}\rangle &= \frac{\gamma_0'}{1-\rho^T\rho+\sigma^2/w_I}\left(1-\left(\frac{\gamma_1'}{\gamma_0'}\right)^2 \times \left[1-\mu\left(w_I(1-\rho^T\rho)+\sigma^2\right)\right]^n\right) \\
&\xrightarrow[n\to\infty]{} \frac{\gamma_0'}{1-\rho^T\rho+\sigma^2/w_I} \\
\langle \bar{\mathbf{c}}(n), \mathbf{V_{1v}}\rangle &= \frac{\gamma_1'}{1-\rho^T\rho+\sigma^2/w_I} \times \left(1-\left[1-\mu\left(w_I(1-\rho^T\rho)+\sigma^2\right)\right]^n\right) \\
&\xrightarrow[n\to\infty]{} \frac{\gamma_1'}{1-\rho^T\rho+\sigma^2/w_I} \\
\langle \bar{\mathbf{c}}(n), \mathbf{V_{iv}}\rangle &= 0, \qquad \text{for } 2\le i\le N-1
\end{aligned} \quad (6)$$

In Sections IV-B and IV-C we examine these projections on simulations of the gradient algorithm for various interference powers and step sizes.

We note two important convergence anomalies which become evident using the subspace analysis. The first is the extreme difficulty of the algorithm to converge, and possibly diverge, when only a small interference power is present. This anomaly is explained by the very weak convexity of the MOE for weak interferers, as demonstrated in Fig. 3. While the algorithm will not be trapped by local minima, it is easily lead astray by spurious noise samples.

In Section IV-C, shown by Fig. 8(d)–(f), we simulate the stochastic gradient and project the detector energy onto the three subspaces Γ_E, $\Gamma_{I\&N}$, and Γ_{NO}. As the interference power diminishes, we see a more and more significant portion of the detector energy appearing in Γ_{NO}. This corresponds to a large component of the detector output being attributable to noise only. While [1] and [5] alluded to the inefficiency of the gradient and the desirability of switching quickly to a decision-directed LMS detector, we now see that when the interference power is weak it is unlikely that the gradient will ever produce meaningful output. We note that the separation of Γ_{act} into Γ_E and $\Gamma_{I\&N}$ was possible due to the special nature of the narrow-band interference, that is, that the interferers were mutually orthogonal. However, the sensitivity of the algorithm to weak multiple-access interference results from the power in subspace Γ_{NO}, a subspace which is the same for wide-band interference in a true CDMA system.

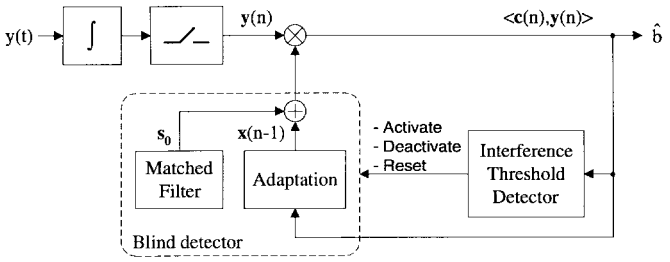

Fig. 5. Proposed adaptive receiver.

The second anomaly we highlight is the possible divergence of the algorithm when allowed to operate indefinitely. The gradient is always sensitive to a large noise sample. The longer the algorithm is allowed to run, the more likely that an outlier noise sample will occur and force the gradient to follow the noise into the space Γ_{NO}. Once displaced into Γ_{NO}, the algorithm has great difficulty in returning to Γ_E. This problem is alluded to in [8], where a step size that shrinks as one over the iteration number is suggested to effectively stop adaptation after a certain point.

In view of these anomalies, we propose a new detector which takes advantage of the new step size for quicker convergence while avoiding adaptation when the interference power is weak. A functional block diagram of the proposed receiver is given in Fig. 5. There are two factors that determine the algorithm's continuing adaptation: iteration number and interference power. When the interference power is very weak, i.e., undetected, the MF is nearly optimal and the control forces the receiver to the MF.

If the interference power is strong, the algorithm has a good chance of converging to the MMSE receiver. In this region the MMSE detector is closely approximated by the decorrelating receiver, and will effectively be converging to the decorrelating detector. Once enough iterations have passed for convergence, we average over several dozen bits to find the mean value for the tap weights and use this as a fixed receiver (alternately, we could use this as the initial state for a decision-directed version of the LMS algorithm). If the interference power degrades significantly we also stop the adaptation, as the likelihood of drifting out of Γ_E and into Γ_{NO} is quite great. We will see in the next section the results of simulations using the proposed receiver.

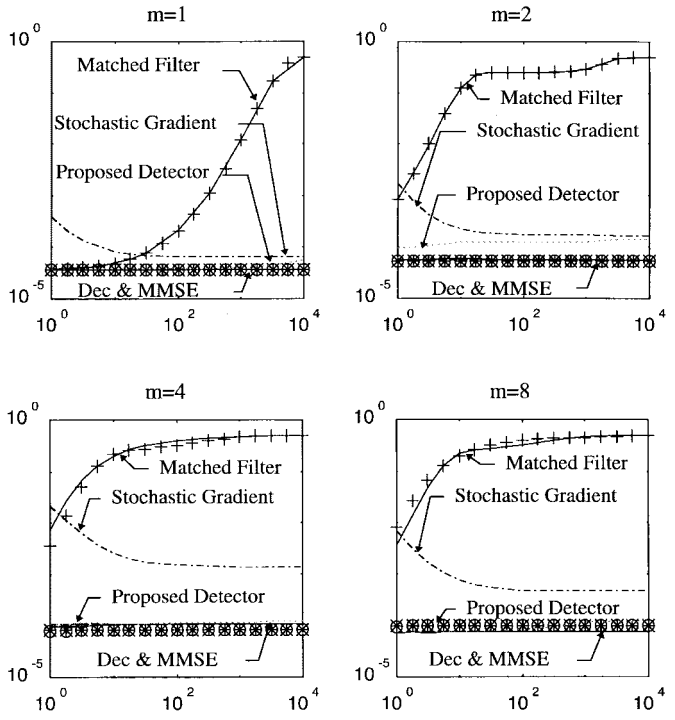

Fig. 6. Probability of error is plotted versus the near–far ratio for various values of m, and several receivers; theoretical values as points, simulation values as curves.

IV. Simulation Results

We present simulation results that confirm theoretical results for probability of error for the fixed receivers. We also trace the tap weight trajectory to show that the adaptive receiver lies in the subspace Γ_E. Simulations also demonstrate much faster convergence when using the new step size found in Section III-C. We confirm by simulation the algorithm's sensitivity to low interference power. In this case, the adaptive receiver is seen to project significant signal energy onto the space of noise only.

A. Monte Carlo versus Theoretical Results

In Fig. 6 we present Monte Carlo simulation results versus the theoretical calculations of the probability of error for three fixed receivers: the MF, the decorrelating detector (DEC), and the MMSE detector. All simulations use an m-sequence of length 63 for the true spread spectrum user, a noise power 6 dB down from the despread CDMA signal (as proposed in [2] during field trials), interference powers that vary from parity with the CDMA signal to 40 dB stronger, and values for m of 1, 2, 4 and 8. We see that simulation and theory match well. The decorrelating and MMSE detectors yield very similar performance.

Fig. 6 also shows results for the stochastic gradient and the new receiver (unless otherwise indicated the old step size is used). For most plots the proposed receiver achieves the performance of the decorrelating or MMSE detector. The gradient's performance improves as the interference power increases. To arrive at reliable estimates of the probability of error it was necessary to run the algorithm for millions of bits.

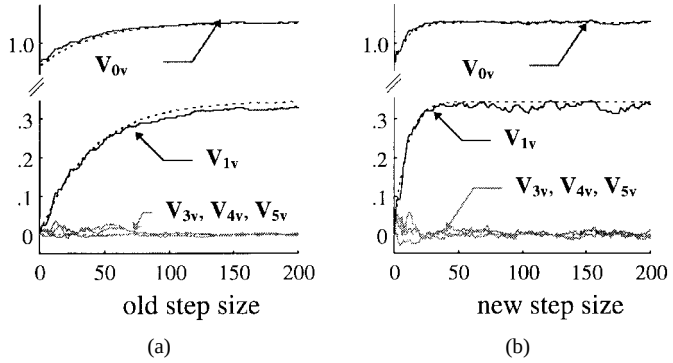

Fig. 7. Projection of tap weights along eigenvectors is plotted versus iteration number for the old and the new adaptation step size.

This allowed adequate opportunity for the gradient algorithm to be lead astray by noise and significantly differ from the MMSE detector, even for very strong interference. Contrast this with the proposed detector. This detector ran adaptively at an interference power of 30 dB for 1000 iterations. The tap weight values were then averaged over the last 100 iterations, a reasonable approach assuming a slowly varying channel. This receiver (now fixed) was used to calculate the probability of error for the range of interference powers. At the time that the gradient algorithm was stopped, it had formed a good estimate of the MMSE detector (noise outliers being unlikely in so few samples).

B. Convergence Time with New Step Size

We next examine the effect on convergence time of the new step-size constraint presented in (5) as opposed to the old criteria proposed in [1] and [5]. Fig. 7 presents curves for the theoretical values of the mean tap weight versus Monte Carlo simulations for an interference power of 30 dB and $m = 4$. We project the tap weights as proposed in (6) onto the subspaces Γ_E and $\Gamma_{\mathrm{I\&N}}$. It is clear that the new step size allows convergence in dozens of iterations, versus hundreds of iterations for the old step size. Given that we wish to switch out of the stochastic gradient adaptation as soon as possible, the new step-size criteria is an important improvement to the algorithm. Note, though, that we also see in these plots the additional excess noise caused by the faster convergence.

C. MOE—Simulation versus Theory

In the next figures we examine the sensitivity of the gradient algorithm to the interference power via simulation. As in the previous section, we project the tap weights as proposed in (6) and plot the simulation projections versus the theoretical values. In Fig. 8(a)–(c) we project along $\mathbf{V_{0v}}$ and $\mathbf{V_{1v}}$ in Γ_E and $\mathbf{V_{2v}}$, $\mathbf{V_{3v}}$, and $\mathbf{V_{4v}}$ in $\Gamma_{I\&N}$. In Fig. 8(a) we have a very weak interferer, 10 dB down from the CDMA signal, and we see that the gradient vector is not able to follow the theoretical mean values. In Fig. 8(b) we have a stronger interferer, 10 dB up from the CDMA signal, and the gradient follows the theoretical mean values more closely but still varies significantly from the optimal values. In Fig. 8(c) we have a strong interferer, 30 dB up from the CDMA signal, and

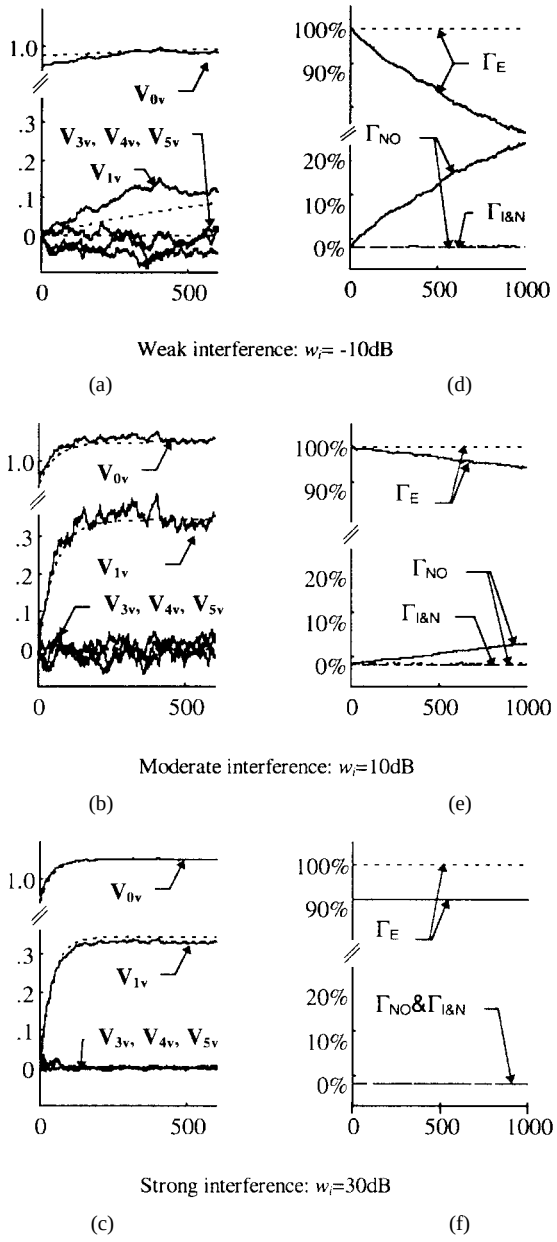

Fig. 8. (a)–(c) Projection of tap weights along eigenvectors is plotted versus iteration number for various near–far ratios and (d)–(f) projection of the receiver output energy onto eigenspaces is plotted versus iteration number for various near–far ratios; theoretical values as dashed lines and simulation values as solid lines.

the gradient attains the optimal tap weights. This is consistent with the anomaly discussed in Section III-C.

In Fig. 8(d)–(f) we present the same simulations, this time projecting the energy onto the three subspaces Γ_E, $\Gamma_{I\&N}$, and $\Gamma_{\rm NO}$. Only the energy in Γ_E can be attributed to the desired signal, and energy in $\Gamma_{\rm NO}$ can only come from the AWGN. In these graphs it is evident that for weak interference the gradient algorithm is tracking noise samples and not the desired user.

V. Conclusion

We apply multiuser detection theory, intended for wide-band interference suppression, to the problem of narrow-band interference suppression in DSSS. We modeled the narrow-band interference as a virtual CDMA system of $m+1$ users. By examining the eigenspace of the received signal we exploited the special form of the narrow-band interference (orthogonal subset of CDMA users) to uncover a two-dimensional subspace Γ_E. This is an unexpected result as in a general system of $m+2$ users, Γ_E would have dimension $m+2$. This subspace is of key importance as all of the signal energy is contained in this subspace while only portions of the interference and noise energies are present. We investigated the performance of three fixed receivers and two adaptive receivers, adopting a subspace approach for the analysis. We demonstrate that the receivers investigated project the received signal onto the subspace Γ_E. We showed that the adaptive version of the MMSE receiver is, on average, constrained to this subspace. This allowed us to identify less restrictive stability constraints on the adaptation step size. We also explain why, for weak interference, the adaptive algorithm is susceptible to outlier noise samples which lead the adaptive receiver to leave the plane Γ_E. We presented simulation results to support these results. Finally, we proposed a new adaptive receiver that avoids the convergence anomalies while capitalizing on the new step size for faster convergence.

Appendix A
Eigenvalues and Eigenvectors of $\mathbf{R_{yy}}$

The matrix $\mathbf{R_{yy}}$ is symmetric and nonnegative definite. Therefore, all eigenvalues are nonnegative and all eigenvectors are orthogonal. By definition, $\Gamma_{\rm act}$ is invariant by $\mathbf{R_{yy}}$ (or $\mathbf{R_{yy}}$-invariant) if for every vector $\mathbf{V} \in \Gamma_{\rm act}$ we find that the transformed vector $\mathbf{R_{yy}V} \in \Gamma_{\rm act}$. $\Gamma_{\rm act}$ is spanned by the signatures. Therefore, we calculate $\mathbf{R_{yy}s}_i$ for $i = 0, \cdots, m+1$

$$\mathbf{R_{yy}s}_0 = (w_0 + \sigma^2)\mathbf{s}_0 + w_I \sum_{i=1}^{m+1} \rho_i \mathbf{s}_i$$

$$\mathbf{R_{yy}s}_i = w_0 \rho_i \mathbf{s}_0 + (w_I + \sigma^2)\mathbf{s}_i, \qquad 1 \le i \le m+1.$$

Note that each signature vector is transformed by $\mathbf{R_{yy}}$ to a linear combination of the signature vectors. Let $\tilde{\mathbf{R}}_{\mathbf{yy}}$ be the restriction of $\mathbf{R_{yy}}$ in $\Gamma_{\rm act}$ so that

$$\mathbf{R_{yy}}[\mathbf{s}_0 \ \cdots \ \mathbf{s}_{m+1}] = [\mathbf{s}_0 \ \cdots \ \mathbf{s}_{m+1}]\tilde{\mathbf{R}}_{\mathbf{yy}}.$$

Using the basis of signature sequences we can write $\tilde{\mathbf{R}}_{\mathbf{yy}}$ in an arrow structure as

$$\tilde{\mathbf{R}}_{\mathbf{yy}} = \begin{bmatrix} w_0 + \sigma^2 & w_0 \rho^T \\ w_I \rho & (w_I + \sigma^2)\mathbf{I_{m+1}} \end{bmatrix}_{B_s}.$$

For every $\mathbf{V} \in \Gamma_{\rm NO}$ we have $\mathbf{R_{yy}V} = \sigma^2\mathbf{V}$, which means that $\Gamma_{\rm NO}$ is $\mathbf{R_{yy}}$-invariant and the matrix $\sigma^2\mathbf{I}_{N-(m+2)}$ is the restriction of $\mathbf{R_{yy}}$ in $\Gamma_{\rm NO}$. Since the eigenvalues of $\mathbf{R_{yy}}$ are the same as those of its restrictions $\tilde{\mathbf{R}}_{\mathbf{yy}}$ and $\sigma^2\mathbf{I}_{N-(m+2)}$, we focus on these matrices. The eigenvalues of $\tilde{\mathbf{R}}_{\mathbf{yy}}$ are equal to the first $(m+2)$ eigenvalues of $\mathbf{R_{yy}}$. We calculate directly the characteristic polynomial of $\tilde{\mathbf{R}}_{\mathbf{yy}}$ defined by

$$P_c(\lambda) = \det(\tilde{\mathbf{R}}_{\mathbf{yy}} - \lambda \mathbf{I_{m+2}})$$

where λ is an eigenvalue and $\mathbf{I_{m+2}}$ is the identity matrix with dimension $m+2$. The matrix $\tilde{\mathbf{R}}_{\mathbf{yy}} - \lambda\mathbf{I_{m+2}}$ also has an arrow

structure

$$\tilde{\mathbf{R}}_{\mathbf{yy}} - \lambda \mathbf{I}_{\mathbf{m+2}} = \begin{bmatrix} w_0 + \sigma^2 - \lambda & w_0 \rho^T \\ w_I \rho & (w_I + \sigma^2 - \lambda)\mathbf{I}_{\mathbf{m+1}} \end{bmatrix}_{B_s}.$$

After row elimination, we arrive at the lower triangular matrix form shown at the bottom of the page, which yields the following characteristic polynomial:

$$P_c(\lambda) = ((w_0 + \sigma^2 - \lambda)(w_I + \sigma^2 - \lambda) - w_I w_0 \rho^T \rho)(w_I + \sigma^2 - \lambda)^m$$

The eigenvalues which solve this polynomial are

$$\lambda_{0y} = \frac{1}{2}(w_0 + w_I + 2\sigma^2 + \sqrt{\phi}),$$
$$\phi = (w_0 - w_I)^2 + 4 w_0 w_I \rho^T \rho$$
$$\lambda_{1y} = \frac{1}{2}(w_0 + w_I + 2\sigma^2 - \sqrt{\phi})$$
$$\lambda_{iy} = w_I + \sigma^2, \qquad 2 \le i \le m+1.$$

Clearly, the eigenvalues of $\mathbf{R}_{\mathbf{yy}}$ arising from the restriction $\sigma^2 \mathbf{I}_{N-(m+2)}$ are

$$\lambda_{iy} = \sigma^2, \qquad m+2 \le i \le N-1.$$

We define $\mathbf{V_{0y}} = [v_0 \quad v_1 \quad \cdots \quad v_{m+1}]^T$ as the eigenvector relative to the eigenvalue λ_{0y} which solves

$$(\tilde{\mathbf{R}}_{\mathbf{yy}} - \lambda_{0y} \mathbf{I}_{\mathbf{m+2}}) \mathbf{V_{0y}} = 0.$$

We arrive at the following system of $m+2$ equations:

$$\begin{aligned} (w_0 - w_I - \sqrt{\phi}) v_0 + 2 w_0 \sum_{i=1}^{m+1} \rho_i v_i &= 0 \\ 2 w_I \rho_i v_0 + (w_I - w_0 - \sqrt{\phi}) v_i &= 0, \qquad 1 \le i \le m+1. \end{aligned} \tag{7}$$

After simplifying we get the single variable equation $(\phi - \phi)v_0 = 0$. It is sufficient to take $v_0 \neq 0$ and, using (7), determine the other components of the eigenvector $\mathbf{V}_{0y}$. The value $v_0 = \frac{1}{2}(w_I - w_0 - \sqrt{\phi})$ offers a simple and compact expression for the other eigenvector components. We proceed similarly to find the second eigenvector $\mathbf{V}_{1y}$ relative to λ_{1y}. After some manipulation, we get the following compact normalized form of the two eigenvectors in the signature basis B_s for Γ_{act}:

$$\mathbf{V_{0y}} = \gamma_0 [\Delta^- \quad -\rho^T]^T_{B_s} \quad \text{and} \quad \mathbf{V_{1y}} = \gamma_1 [\Delta^+ \quad -\rho^T]^T_{B_s}$$

where

$$\Delta^{\pm} = \frac{1}{2}\left(1 - \alpha^{-2} \pm \sqrt{(1-\alpha^{-2})^2 + 4\alpha^{-2}\rho^T\rho}\right), \qquad \alpha = \sqrt{w_I / w_0}$$

and

$$\gamma_0 = ((\Delta^- - \rho^T\rho)^2 + \rho^T\rho(1 - \rho^T\rho))^{-1/2}$$
$$\gamma_1 = ((\Delta^+ - \rho^T\rho)^2 + \rho^T\rho(1 - \rho^T\rho))^{-1/2}.$$

It is important to note that the nature of $\mathbf{V_{0y}}$ and $\mathbf{V_{1y}}$ allows us to form the linear combination

$$\begin{aligned} \gamma_1^{-1}\mathbf{V_{1y}} - \gamma_0^{-1}\mathbf{V_{0y}} &= (\Delta^+ - \Delta^-)[1 \quad 0 \quad \cdots \quad 0]_{B_s} \\ &= (\Delta^+ - \Delta^-)\mathbf{s_0} \end{aligned}$$

which implies that $\mathbf{s_0}$ can be expressed as a linear combination of $\mathbf{V_{0y}}$ and $\mathbf{V_{1y}}$

$$\begin{aligned} \mathbf{s_0} &= \frac{1}{\Delta^+ - \Delta^-}\left(\gamma_1^{-1}\mathbf{V_{1y}} - \gamma_0^{-1}\mathbf{V_{0y}}\right) \\ &= \frac{\alpha^2}{\sqrt{(\alpha^2-1)^2 + 4\alpha^2\rho^T\rho}}\left(\gamma_1^{-1}\mathbf{V_{1y}} - \gamma_0^{-1}\mathbf{V_{0y}}\right). \end{aligned}$$

The decorrelating detector for the virtual CDMA system is given in [6] as $\mathbf{c_{DEC}} = [1 \quad -\rho^T]^T_{B_s}$. The form of $\mathbf{V}^{\perp}$ and $\mathbf{c_{DEC}}$ allows us to write the following linear combination:

$$\mathbf{c_{DEC}} = \sqrt{\rho^T\rho(1-\rho^T\rho)} \cdot \mathbf{V}^{\perp} + (1 - \rho^T\rho)\mathbf{s_0}.$$

To arrive at the canonical form of the decorrelating detector we normalize with respect to $\langle \mathbf{s_0}, \mathbf{c_{DEC}} \rangle$

$$\begin{aligned} \mathbf{c_{DEC}} &= \frac{1}{\sqrt{1-\rho^T\rho}} \cdot [1, \quad -\rho^T]^T_{B_s} \\ &= \mathbf{s_0} + \sqrt{\frac{\rho^T\rho}{1-\rho^T\rho}} \cdot \mathbf{V}^{\perp} = \mathbf{s_0} + \beta_{\text{DEC}} \cdot \mathbf{V}^{\perp}. \end{aligned}$$

The system of linear equations describing the eigenspace relative to the third eigenvalue is

$$\sum_{i=1}^{m+1} \rho_i v_i = 0, \quad v_0 = 0$$

which defines an m-dimensional convex hyperplane. We choose

$$V_{2y} = [0 \quad \rho_2\rho_1 \quad -\rho_1^2 \quad 0 \quad \cdots \quad 0]^T_{B_s} \left(\rho_1^2(\rho_1^2 + \rho_2^2)\right)^{-1/2}$$

which solves the simple equation $\rho_1 v_1 + \rho_2 v_2 = 0$. The next eigenvector can be determined iteratively; it must verify the two conditions

$$\langle \mathbf{V_{3y}}, \mathbf{V_{2y}} \rangle = 0$$
$$\rho_1 v_1 + \rho_2 v_2 + \rho_3 v_3 = 0.$$

In such a way, all of the orthonormal eigenvectors relative to the eigenspace $\Gamma_{\text{I\&N}}$ have the form

$$V_{iy} = [0 \quad \rho_i\rho_1 \quad \cdots \quad \rho_i\rho_{i-1} \quad \delta_i \quad 0 \quad \cdots \quad 0]^T_{B_s} \gamma_i$$

$$(w_I + \sigma^2 - \lambda)[\tilde{\mathbf{R}}_{\mathbf{yy}} - \lambda \mathbf{I}_{\mathbf{m+2}}] = \begin{bmatrix} (w_0 + \sigma^2 - \lambda)(w_I + \sigma^2 - \lambda) - w_I w_0 \rho^T \rho & w_I \rho^T \\ 0 & (w_I + \sigma^2 - \lambda)\mathbf{I}_{\mathbf{m+1}} \end{bmatrix}_{B_s}$$

where

$$\delta_i = -\sum_{j=1}^{i-1} \rho_j^2,$$

and

$$\gamma_i^{-1} = \sqrt{\left(\sum_{j=1}^{i-1} \rho_j^2\right)\left(\sum_{j=1}^{i} \rho_j^2\right)}, \qquad 2 \le i \le m+1.$$

It is important to note that all of the above $m-1$ vectors are orthogonal to the real CDMA signature $\mathbf{s_0}$. The remaining $N-m-1$ eigenvectors of the covariance matrix $\mathbf{R}_{yy}$ relating to the remaining eigenvalues $\lambda_{iy} = \sigma^2,\ i = m+2, \cdots, N$ can be easily determined by combining the above $m+1$ eigenvectors and the standard basis vectors, and using the Gram–Schmidt orthogonalization.

We note that the MOE can be written as a single variable function. To find the value β which minimizes the MOE, we differentiate

$$\frac{\partial \mathrm{MOE}(\beta)}{\partial \beta} = 2\beta(w_I(1-\rho^T\rho)+\sigma^2) - 2w_I\sqrt{\rho^T\rho(1-\rho^T\rho)}$$

to arrive at

$$\beta_{\min} = \frac{\sqrt{\rho^T\rho(1-\rho^T\rho)}}{1-\rho^T\rho+\sigma^2/w_I}.$$

We can easily verify that this is a minimum by examining the second derivative of MOE

$$\frac{\partial^2 \mathrm{MOE}(\beta)}{\partial^2 \beta} = 2(w_I(1-\rho^T\rho)+\sigma^2) \ge 0 \quad \forall \beta.$$

Appendix B
Eigenvalues and Eigenvectors of $\mathbf{R_{vy}}$

Similarly as in Appendix A, we demonstrate that Γ_{act} is $\mathbf{R_{vy}}$-invariant and we determine the restriction $\tilde{\mathbf{R}}_{\mathbf{vy}}$ of $\mathbf{R_{vy}}$ in Γ_{act}. We calculate the eigenvalues and eigenvectors of $\mathbf{R_{vy}}$ using the same method as in Appendix A, and note that the eigenvalues were simultaneously reported in [5]. In the basis B_s we obtain the special arrow structure

$$\tilde{\mathbf{R}}_{\mathbf{vy}} = \begin{bmatrix} -w_I\rho^T\rho & -(w_I+\sigma^2)\rho^T \\ w_I\rho & (w_I+\sigma^2)I_{\mathbf{m+1}} \end{bmatrix}_{B_s}.$$

After column elimination, we arrive at the upper triangular matrix, shown at the bottom of the page, which yields the characteristic polynomial

$$P_c(\lambda) = -\lambda(w_I(1-\rho^T\rho)+\sigma^2-\lambda)(w_I+\sigma^2-\lambda)^m.$$

The eigenvalues which solve this characteristic polynomial are

$$\lambda_{0v} = 0$$
$$\lambda_{1v} = w_I(1-\rho^T\rho)+\sigma^2$$
$$\lambda_{iv} = w_I+\sigma^2 \quad \text{multiplicity } m.$$

Similarly as in Appendix A, we demonstrate that Γ_{NO} is $\mathbf{R_{vy}}$-invariant and we determine the restriction $\tilde{\mathbf{R}}_{\mathbf{vy}}$ of $\mathbf{R_{vy}}$ in Γ_{NO}. The eigenvalues of $\mathbf{R_{vy}}$ assigned to Γ_{NO} are

$$\lambda_{iv} = \sigma^2 \quad \text{multiplicity } N-m-2.$$

We note that the matrix $\mathbf{R_{vy}}$ can be expressed as

$$\mathbf{R_{vy}} = (\mathbf{I_N} - \mathbf{s_0}\mathbf{s_0^T})\mathbf{R_{yy}}.$$

The matrix $\mathbf{I}_N - \mathbf{s}_0\mathbf{s}_0^T$ is well described in Householder's book [9]. In fact, it defines a projection of the N-dimensional space along the $\mathbf{s}_0$ direction. The matrix $\mathbf{I}_N - \mathbf{s}_0\mathbf{s}_0^T$ has these important properties.

1. If $\mathbf{V} \perp \mathbf{s}_0$, then $(\mathbf{I}_N - \mathbf{s}_0\mathbf{s}_0^T)\mathbf{V} = \mathbf{V}$ for any $\mathbf{V} \in \Gamma$.
2. If $\mathbf{V}//\mathbf{s}_0$, then $(\mathbf{I}_N - \mathbf{s}_0\mathbf{s}_0^T)\mathbf{V} = 0$.

These properties allow us to conclude

$$\begin{aligned} \mathbf{s_0} \perp \Gamma_{I\&N} &\Rightarrow \left\langle (\mathbf{I_N} - \mathbf{s_0}\mathbf{s_0^T}), \Gamma_{I\&N} \right\rangle = \Gamma_{I\&N} \\ &\Rightarrow \mathbf{V_{iv}} = \mathbf{V_{iy}} \quad \text{for } 2 \le i \le m+1 \\ \mathbf{s_0} \perp \Gamma_{\mathrm{NO}} &\Rightarrow \left\langle (\mathbf{I_N} - \mathbf{s_0}\mathbf{s_0^T}), \Gamma_{\mathrm{NO}} \right\rangle = \Gamma_{\mathrm{NO}} \\ &\Rightarrow \mathbf{V_{iv}} = \mathbf{V_{iy}}, \qquad \text{for } m+2 \le i \le N-1. \end{aligned}$$

The projection matrix $\mathbf{I}_N - \mathbf{s}_0\mathbf{s}_0^T$ changes only the two first eigenvectors that span Γ_E. $\mathbf{V_{0v}}$ and $\mathbf{V_{1v}}$ can therefore be determined from $\mathbf{V_{0y}}$ and $\mathbf{V_{1y}}$. The two eigenvectors $\mathbf{V_{0v}}$ and $\mathbf{V_{1v}}$ relate, respectively, to the two eigenvalues λ_{0v} and λ_{1v}, and they span the plane subspace Γ_E. We arrive at

$$\mathbf{V_{0v}} = \frac{1}{\gamma_0'}\left[1 + \frac{\sigma^2}{w_I} - \rho^T\right]_{B_s}^T$$
$$\gamma_0' = \sqrt{\left(1+\frac{\sigma^2}{w_I}\right)^2(1-\rho^T\rho) + \left(\frac{\sigma^2}{w_I}\right)^2\rho^T\rho}$$
$$\mathbf{V_{1v}} = \frac{1}{\gamma_1'}[\rho^T\rho - \rho^T]_{B_s}^T$$
$$\gamma_1' = \sqrt{\rho^T\rho(1-\rho^T\rho)}.$$

The eigenvector $\mathbf{V_{0y}}$ is a normalized version of the MMSE detector. $\mathbf{V_{1y}}$ is equal to $\mathbf{V}^{\perp}$, the normal vector in Γ_E orthogonal to the desired user signature $\mathbf{s_0}$. $\mathbf{s_0}$ can be expressed as linear combination of the eigenvectors $\mathbf{V_{0v}}$ and $\mathbf{V_{1v}}$

$$\mathbf{s_0} = \frac{1}{1-\rho^T\rho+\sigma^2/w_I}(\gamma_0'\mathbf{V_{0v}} - \gamma_1'\mathbf{V_{1v}}).$$

In [5], Poor and Wang defined the matrix $\mathbf{R_{vv}} = (\mathbf{I_N} - \mathbf{s_0}\mathbf{s_0^T})\mathbf{R_{yy}}(\mathbf{I_N} - \mathbf{s_0}\mathbf{s_0^T})$. In order to simplify calculation of the tap weight error correlation matrix, they made the approximation $\mathbf{\Lambda_{yy}} \approx \mathbf{\Lambda_{vy}} \approx \mathbf{\Lambda_{vv}}$ where $\mathbf{\Lambda_{yy}}$, $\mathbf{\Lambda_{vy}}$, and $\mathbf{\Lambda_{vv}}$ are, respectively, the diagonal forms of $\mathbf{R_{yy}}$, $\mathbf{R_{vy}}$, and $\mathbf{R_{vv}}$. We write $\mathbf{R_{vv}} = \mathbf{R_{vy}}(\mathbf{I_N} - \mathbf{s_0}\mathbf{s_0^T})$ and use the properties of the projection matrix to determine the eigenvalues and eigenvectors of $\mathbf{R_{vv}}$.

$$(w_I+\sigma^2-\lambda)[\tilde{\mathbf{R}}_{\mathbf{vy}} - \lambda\mathbf{I_{m+2}}]_{\Gamma_{\mathrm{act}}} = \begin{bmatrix} -(w_I\rho^T\rho+\lambda)(w_I+\sigma^2-\lambda) + w_I(w_I+\sigma^2)\rho^2\rho & -(w_I+\sigma^2)\rho^T \\ 0 & (w_I+\sigma^2-\lambda)\mathbf{I_{m+1}} \end{bmatrix}_{B_s}$$

$\mathbf{R_{vv}}\mathbf{s}_0 = 0$, so $\mathbf{s_0}$ is the first eigenvector of $\mathbf{R_{vv}}$, relative to a zero eigenvalue. All the other eigenvectors of $\mathbf{R_{vy}}$ are orthogonal to $\mathbf{s_0}$ and, therefore, are invariant under the projection matrix $\mathbf{I}_N - \mathbf{s}_0\mathbf{s}_0^T$. $\mathbf{R_{vv}}$ has the same eigenvalues as $\mathbf{R_{vy}}$. We conclude that the approximation made in [5] is partially exact, i.e.,

$$\Lambda_{\mathbf{yy}} \neq \Lambda_{\mathbf{vy}} = \Lambda_{\mathbf{vv}}.$$

REFERENCES

[1] M. Honig, U. Madhow, and S. Verdú, "Blind adaptive multiuser detection," *IEEE Trans. Inform. Theory*, vol. 41, pp. 944–960, July 1995.

[2] L. B. Milstein, D. L. Schilling, R. Pickholz, V. Erceg, M. Kullback, E. G. Kanterakis, D. S. Fishman, W. H. Biederman, and D. C. Salerno, "On the feasibility of a CDMA overlay for personal communications networks," *IEEE J. Select. Areas Commun.*, vol. 10, pp. 655–668, May 1992.

[3] L. B. Milstein, "Interference rejection techniques in spread spectrum communications," in *Proc. IEEE*, vol. 76, pp. 657–671, June 1988.

[4] L. A. Rusch and H. Fathallah, "MMSE detector for narrow-band interference suppression in DS spread spectrum," in *Interference Rejection and Signal Separation in Wireless Communications Symp.*, Newark, NJ, Mar. 19, 1996, pp. 147–163.

[5] H. V. Poor and X. Wang, "Adaptive suppression of narrow-band digital interferers from spread spectrum signals," *Special Issue on Interference of Wireless Personal Communications in Mobile Wireless Systems*, to be published.

[6] L. A. Rusch and H. V. Poor, "Multiuser detection techniques for narrow-band interference suppression in spread spectrum," *IEEE Trans. Commun.*, vol. 43, pp. 1725–1745, Apr. 1995.

[7] S. Verdú and J. B. Thomas, *Multiuser Detection*. Greenwich, CT: JAI Press, 1993.

[8] U. Madhow and M. L. Honig, "MMSE interference suppression for direct-sequence spread-spectrum CDMA," *IEEE Trans. Commun.*, vol. 42, pp. 3178–3188, Dec. 1994.

[9] A. S. Householder, *The Theory of Matrices in Numerical Analysis*, 1st ed. London, U.K.: Blaisdell, 1964.

Habib Fathallah (S'96) was born in Ras Jebel, Tunisia, on March 14, 1969. He received the B.S. and M.S. degrees (with honors) in electrical engineering from the National Engineering School of Tunis, Tunisia, in 1994, and the second M.S.E.E. degree in CDMA wireless communications from l'Université Laval, P.Q., Canada, in 1997. He is currently pursuing the Ph.D. degree at the Centre d'Optique Photonique et Laser (COPL), l'Université Laval.

His research interests include CDMA optical local area networks and wireless communications.

Leslie A. Rusch (S'91–M'94) was born in Chicago, IL. She received the B.S.E.E. degree from the California Institute of Technology, Pasadena, CA, in 1980, and the M.A. and Ph.D. degrees in electrical engineering from Princeton University, Princeton, NJ, in 1992 and 1994, respectively.

She is currently with l'Université Laval, P.Q., Canada, as an Assistant Professor of Electrical Engineering. She occupies a chair in optical communications jointly sponsored by the Natural Science and Engineering Research Council of Canada and Québec-Téléphone. Her research interests include fiber optic communications, transient gain analysis of erbium-doped fiber amplifiers, wireless communications, spread spectrum communications, and CDMA for radio and optical frequencies.